energies

MDPI

Article

An Analytical Model for Lithium Storage in Spherical Fullerenes

Mansoor H. Alshehri

Department of Mathematics, College of Science, King Saud University, P.O. Box 2455, Riyadh 11451, Saudi Arabia; mhalshehri@ksu.edu.sa

Abstract: In this paper, the encapsulation of lithium atoms in spherical fullerenes of varying sizes is investigated. The 6–12 Lennard–Jones potential function and the continuum approximation, in which it is assumed that the atoms can be replaced with a uniform distribution across the surface of the molecules, are exploited to model the interaction energies between lithium atoms and spherical fullerenes. Thus, the total interaction energies can be approximated by applying surface integrations. The results show that for a lithium atom interacting inside a spherical fullerene, the interaction energies are minimized at a position that approaches the fullerene wall as the size of the fullerene increases. However, the results show that an external force would need to be applied to a lithium atom in order to overcome the repulsive energy barrier so that it can be encapsulated in C_N fullerenes with a radius of less than 2 Å. The present study indicates that the optimal radius that gives the minimum energy for the storage of Li inside C_N fullerenes occurs for a fullerene with a radius of $\approx$ 2.4 Å. Overall, this study provides an analytical formulation that may facilitate rapid computational results, and an application of this work is in the design of future high-energy-density batteries that utilize C_N fullerenes.

Keywords: lithium; encapsulation; continuum approach; fullerenes; mathematical modeling

check for updates

Citation: Alshehri, M.H. An Analytical Model for Lithium Storage in Spherical Fullerenes. *Energies* **2022**, *15*, 7154. https://doi.org/10.3390/en15197154

Academic Editors: Saeid Gholami Farkoush, Sang-Bong Rhee, Sanam SaeidNahaei, Tahir Khurshiad and Abdul Wadood

Received: 7 September 2022
Accepted: 26 September 2022
Published: 28 September 2022

1. Introduction

Carbon is fundamental for all of organic chemistry, it is an element that is abundant in nature, and it can be found on Earth in massive amounts; in addition, elemental carbon can be cheaply produced through suitable conversion reactions [1]. The discovery of carbon nanostructures, such as nanotubes, nanotori, nano-onions, nanobundles, and fullerenes, has generated considerable research into their potential applications and properties [2–4]. Fullerenes are a class of carbon nanomaterials, and they were discovered by a research group at Rice University in 1985 [5]; they may have several electronic, semiconducting, and biomedical applications. In addition, due to their electronic properties that arise from their large surface-to-volume ratio and their mechanical properties that arise from van der Waals (vdW) forces, fullerenes have revolutionized many technologies through their properties as potent radical scavengers, excellent electron acceptors, and antioxidants, and they might make possible the creation of many future nanoscale devices [3,6,7]. On the other hand, lithium (Li) metal has a high energy density and highly reactive chemical characteristics that cause it to require stringent environmental requirements for its processing, conservation, and utilization [8]. Carbon nanostructures are candidate materials for meeting the requirements of rechargeable lithium batteries due to such properties as their appropriately high specific surface area, outstanding hierarchical architecture, high electrical conductivity, high thermal stability, low cost, and environmental benignity. Li@C_N composites may be used as new nanomaterials that offer a very high ionic conductivity that is better than that of empty fullerenes, and they are likely to have many applications in organic and dye-sensitized solar cells. Furthermore, carbon nanomaterials—including fullerenes—might be used as new alternative anode materials that contain lithium due to their strong covalent bonds with low ionicity, which can support large bandwidths [1]. In addition, the mobilities of lithium ions and electrons in carbon nanostructures—including fullerenes—are quite substantial, resulting in a comparatively high chemical diffusion coefficient of lithium [1,9]. Fullerenes might offer the necessary characteristics to make them attractive anode materials in lithium-based batteries; these characteristics include the high chemical potential of lithium in lithiated compounds, the high capacity for lithium, the small changes in volume during extraction/insertion, and the fast lithium extraction/insertion kinetics. In addition, they can be chemically bonded with other molecules without experiencing changes in their electronic properties [1,10]. Many experiments have been conducted to study the storage of lithium inside fullerenes and to improve the cyclic performance of recharging. Bai et al. used first-principle density-functional theory (DFT) calculations to examine the encapsulation of a single lithium atom inside C_N fullerenes with various cage sizes (N = 20–70); they used one structure for each fullerene to capture an Li atom [8]. They showed that the values of the interaction energies for Li@C_N are all negative, which means that the encapsulation process of Li@C_N is energetically favorable. In addition, their results showed that the energy values became more negative for C_{30}. An et al. examined the electronic and geometrical properties of Li@C_{20}, and they found that Li@C_{20} is energetically stable and has strong total magnetic moments [11]. Moreover, Stefanou et al. combined time-dependent density-functional theory (TDDFT) calculations, gas-phase Rydberg photoelectron spectroscopy, and low-temperature scanning tunneling spectroscopy (STS) to study isolated Li@C_{60}. They found that the most energetically favorable configuration was when the displacement of the Li atom is 1.54 Å from the center of a C_{60} fullerene [12]. Debnath et al. used DFT calculations to study the geometrical, electronic, and thermodynamic properties of Li@C_N fullerenes, where N = 20, 32, 42, and 60 [13]. Their results for the smallest fullerene C_{20} showed that only one Li atom could be encapsulated in a C_{20} fullerene, while C_{32} could encapsulate two Li atoms, and C_{42} could encapsulate three Li atoms; the number of Li atoms that could be encapsulated inside a C_{60} fullerene was 7–9. Computational simulation and mathematical modeling play important roles in predicting and verifying experimental outcomes, which can often be expensive and time consuming. However, the main advantage of the method used here is the derivation of analytical expressions from which the numerical solutions for various physical scenarios might be readily determined. As demonstrated in Figure 1, the encapsulation of lithium atoms inside C_N fullerenes is investigated; the major target of this study is an optimal fullerene that requires minimal energy for the storage of a lithium atom inside the fullerene.The interactions of Li atoms inside fullerene molecules are determined mathematically by adopting the Lennard–Jones (LJ) function together with the continuum approximation, which can be used to approximate the vdW interactions between lithium atoms and fullerenes.

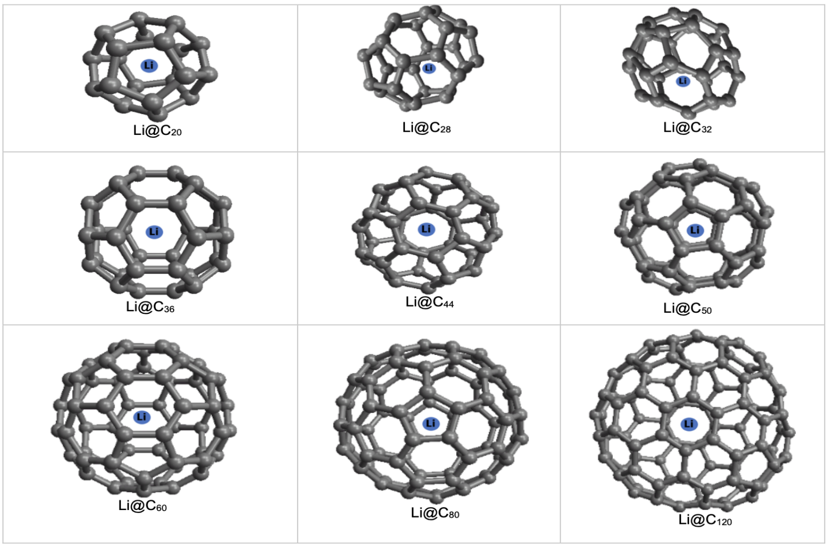

Figure 1. Storage of a Li atom in C_N fullerenes.

2. Mathematical Modeling

The theoretical background for the method used here is summarized in this section. The vdW interactions between non-bonded atoms can be explained by using a mathematical model in order to obtain the physical mechanisms of the interactions of Li atoms inside C_N fullerenes, as shown in Figure 2. As mentioned above, the LJ potential function will be used to model the molecular interactions between Li atoms and fullerenes. The LJ potential function accounts for the interaction of two non-bonded atoms with the distance δ, and this can be written in the form

$$U(\delta) = -\frac{A}{\delta^6} + \frac{B}{\delta^{12}},$$

where A and B denote the LJ attractive and repulsive constants, respectively, and they can be determined using the Lorentz–Berthelot mixing rule [14]. The carbon atoms on the fullerene molecules are assumed to be uniformly distributed over their surfaces; thus, the continuum approximation may be used. So, to find the total interaction energies between the Li atoms and the fullerenes, a surface integration is applied, and this is given by

$$E_{tot} = \ell \int_S U(\delta)\, dS \tag{1}$$

where dS and ℓ are the surface area element and the mean atomic surface density of the fullerene, respectively; for a fullerene with N atoms and radius r, the mean atomic surface density can be calculated using $\ell = N/(4\pi r^2)$.

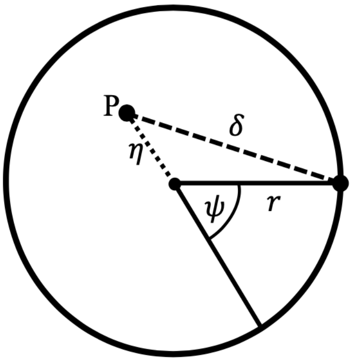

Figure 2. Geometry of a Li atom inside a spherical fullerene.

In this model, an interaction between a spherical surface (a fullerene) and a single point (Li atom) is considered, as shown in Figure 2. The Li atom is located in Cartesian coordinates at a point $P = (0, 0, \eta)$, where η is the distance from the center of the sphere of radius r, which is parametrized in spherical coordinates as (r, ϕ, ψ), where $r \in [0, \infty), \phi \in (0, \pi]$, and $\psi \in [-\pi, \pi]$. To map from the spherical to the Cartesian coordinate system, we have $(r \sin\phi \cos\psi, r \sin\phi \sin\psi, r \cos\phi)$; thus, $\delta^2 = r^2 - 2r\eta\cos\phi + \eta^2$, and the interaction of a point (Li atom) inside a sphere (fullerene) can be given as

$$E_{tot} = r^2 \ell \int_{-\pi}^{\pi} \int_0^{\pi} \left[\frac{-A \sin\phi}{(r^2 - 2r\eta\cos\phi + \eta^2)^3} + \frac{B \sin\phi}{(r^2 - 2r\eta\cos\phi + \eta^2)^6} \right] d\phi\, d\psi.$$

To evaluate these integrals, we introduce the integral I_n, where $(n = 3, 6)$:

$$I_n = r^2 \int_{-\pi}^{\pi} \int_0^{\pi} \left[\frac{\sin\phi}{(r^2 - 2r\eta\cos\phi + \eta^2)^n} \right] d\phi\, d\psi.$$

The integral is independent of ψ, so

$$I_n = 2\pi r^2 \int_0^{\pi} \frac{\sin\phi}{(r^2 - 2r\eta\cos\phi + \eta^2)^n}\, d\phi. \tag{2}$$

Here, the hypergeometric function $F(a^*, b^*; c^*; z)$ can be used to evaluate this integral, so we may rewrite the integral as

$$I_n = 2\pi r^2 \int_0^{\pi} \frac{2\sin(\phi/2)\cos(\phi/2)}{\left[4r\eta\sin^2(\phi/2) + (\eta - r)^2\right]^n}\, d\phi.$$

By making the substitution $w = \sin^2(\phi/2)$, I_n becomes

$$I_n = \frac{4\pi r^2}{(\eta - r)^{2n}} \int_0^1 \left[1 + \frac{4\eta r}{(\eta - r)^2} t\right]^{-n} dw.$$

As we can see, the integral I_n is now in the form of a hypergeometric integral. Here, we use the most useful hypergeometric function, which is Euler's integral formula, and it is given by

$$F(a^*, b^*; c^*; z) = \frac{\Gamma(c^*)}{\Gamma(b^*)\Gamma(c^* - b^*)} \int_0^1 (1 - yz)^{-a^*}(1 - y)^{c^* - b^* - 1} y^{b^* - 1}\, dy,$$

where $\Gamma(\beta)$ is the gamma function, and for the integral I_n, we have $a^* = n, b^* = 1, c^* = 2$, and $z = -4\eta r/(\eta - r)^2$. Therefore,

$$I_n = \frac{4\pi r^2}{(\eta - r)^{2n}} F\left[n, 1; 2; \frac{-4\eta r}{(\eta - r)^2}\right].$$

We can note that $c^* = 2b^*$; therefore, we can use a quadratic transformation from [15], which is given as

$$F(a^*, b^*; c^*; z) = (1 - z)^{-a^*/2} F\left[a^*, 2b^* - a^*; b^* + 1/2; \frac{(1 - \sqrt{1 - z})^2}{4\sqrt{1 - z}}\right].$$

Thus, I_n becomes

$$I_n = \frac{4\pi r^2}{(\eta^2 - r^2)^n} F\left(n, 2 - n; 3/2; \frac{-r^2}{\eta^2 - r^2}\right).$$

Therefore, the total interaction E_{tot} of a Li atom inside a spherical fullerene is given by

$$E_{tot} = \frac{-4A\ell\pi r^2}{(\eta^2 - r^2)^3} F\left(3, -1; 3/2; \frac{-r^2}{\eta^2 - r^2}\right) + \frac{4B\ell\pi r^2}{(\eta^2 - r^2)^6} F\left(6, -4; 3/2; \frac{-r^2}{\eta^2 - r^2}\right).$$

where $A = 4\epsilon\sigma^6 = 0.64$ eVÅ^6 and $B = 4\epsilon\sigma^{12} = 56.16$ eVÅ^{12}, σ is the vdW diameter, and ϵ is the depth of the potential well; their values are taken from [16,17].

An alternative approach:

Here, an alternative approach is used to derive an expression and evaluate the integral I_n as follows:

$$I_n = 2\pi r^2 \int_0^{\pi} \frac{\sin\phi}{(r^2 - 2r\eta\cos\phi + \eta^2)^n}\, d\phi.$$

By using change in variables $u = r^2 - 2r\eta\cos\phi + \eta^2$,

$$\begin{aligned} I_n &= \frac{\pi r}{\eta} \int_{(\eta-r)^2}^{(\eta+a)^2} \frac{du}{u^n} \\ &= \frac{\pi r}{\eta(1-n)} \left[\frac{1}{(\eta-r)^{2(n-1)}} - \frac{1}{(\eta+r)^{2(n-1)}} \right]. \end{aligned}$$

Therefore, using this approach, the total interaction E_{tot} can be given by

$$E_{tot} = \frac{\pi r \ell}{\eta} \left\{ -\frac{A}{2} \left[\frac{1}{(\eta-r)^4} - \frac{1}{(\eta+r)^4} \right] + \frac{B}{5} \left[\frac{1}{(\eta-r)^{10}} - \frac{1}{(\eta+r)^{10}} \right] \right\}. \tag{3}$$

In addition, by using Equation (3), the optimal size of the radius of the fullerene that gives the position with the minimal energy of the Li atom is determined as follows:

$$E_{tot} = \lim_{\eta \to 0} \frac{f'(\eta)}{g'(\eta)} = \frac{-4\pi A}{r^4} + \frac{4\pi B}{r^{10}}.$$

Now, we solve the following equation for r to obtain the critical radius that minimizes E_{tot}

$$\frac{dE_{tot}}{dr} = \frac{16\pi A}{r^5} - \frac{40\pi B}{r^{11}} = 0,$$

and we find that E_{tot} is at its minimum when r satisfies

$$r = \left(\frac{5B}{2A} \right)^{1/6}. \tag{4}$$

3. Discussion and Numerical Results

Here, the numerical results according to the expressions given in the "Mathematical Modeling" section are presented. The storage of a lithium atom inside various C_N fullerenes (N = 20, 28, 32, 36, 44, 50, 60, 80, and 120) is investigated. The calculations were carried out by employing the Maple software together with the physical parameters involved in the model, which are shown in Table 1. The relation between the equilibrium position η and the interactions for a Li atom encapsulated in a spherical fullerene C_N is plotted in Figure 3. Firstly, Figure 3 and Table 2 show that the values of the interaction energy for Li inside C_N are all negative, which indicates that the encapsulation process of Li@C_N is energetically favorable. In addition, the equilibrium distance η between two atoms occurs when the LJ energy is at its minimum, so, from Figure 3, we find that the value of η for the Li atom inside the C_{20}, C_{28}, and C_{32} fullerenes is approximately 0 Å, which means that the Li atom is located at the center of these three fullerenes. For the C_{36}, C_{44}, C_{50}, C_{60}, C_{80}, and C_{120} fullerenes, the values of η are approximately $0.36, 0.68, 1.05, 1.28, 1.81$, and 3.09 Å, respectively, so we can deduce that the position of the Li atom tends to be closer to the wall of the fullerene as the radius of the fullerene becomes larger. Moreover, Figure 4 shows that the lithium atom cannot be stored in a fullerene with a radius of less than ≈ 2, which is because of the increase in the positive energy of the Li atom's interaction with the fullerene due to the lack of space for the encapsulation of the Li atom inside of it.

Table 1. Values of the radius r and the mean atomic surface density ℓ of the C_N fullerenes.

C_N	r (Å)	$\ell = N/4\pi r^2$ (Å^{-2})
C_{20}	2.1 [18,19]	0.371
C_{28}	2.42 [18,19]	0.380
C_{32}	2.63 [18]	0.368
C_{36}	2.80 [18,19]	0.365
C_{44}	3.00 [18]	0.389
C_{50}	3.33 [18]	0.365
C_{60}	3.50 [4]	0.389
C_{80}	4.00 [4]	0.397
C_{120}	5.25 [20]	0.346

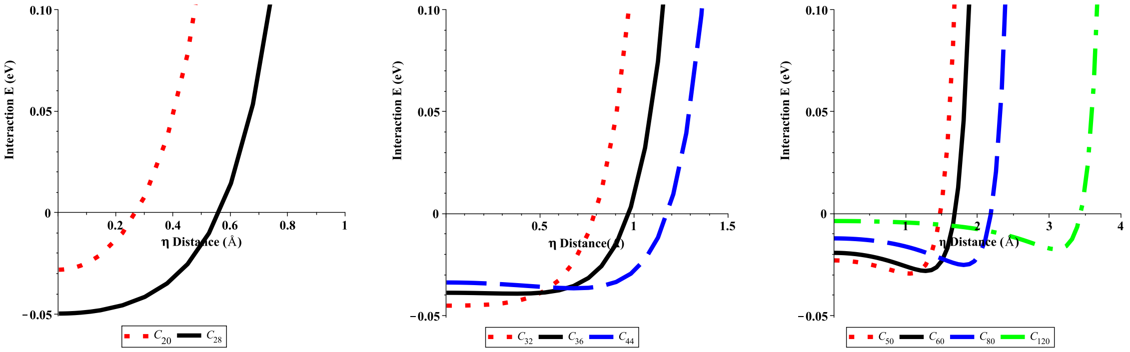

Figure 3. Interaction energies of an offset Li atom inside the C_N fullerenes (N = 20, 28, 32, 36, 44, 50, 60, 80, and 120) with respect to the radial offset distance η from the center of the fullerenes.

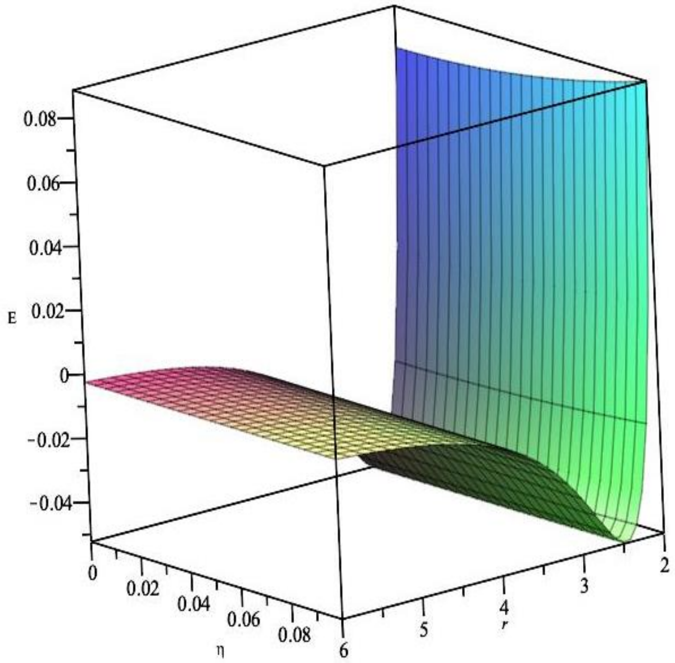

Figure 4. Total energy for a Li atom stored inside a C_N fullerene.

Table 2. Main results of the equilibrium position η and interaction energies E.

C_N	C_{20}	C_{28}	C_{32}	C_{36}	C_{44}	C_{50}	C_{60}	C_{80}	C_{120}
η (Å)	0	0	0	0.37	0.68	1.05	1.28	1.81	3.09
E (eV)	−0.028	−0.048	−0.044	−0.040	−0.35	−0.030	−0.028	−0.024	−0.019

Furthermore, Figure 5 shows the interaction as a function of the radius r of the fullerene. Thus, from Figure 5 and by substituting the values of A and B into Equation (4), the critical radius of the fullerene for which the configuration of the Li atom inside the fullerene results in the minimal interaction energy is obtained at $\eta = 0$. We observe that the preferred radius of the fullerene for enclosing the Li atom is ≈2.4 Å, so we might infer that C_N where N = 28–32 is the preferred fullerene. We comment that our results confirm that an Li atom can be stored inside the C_N fullerenes where N = 20, 28, 32, 36, 44, 50, 60, 80, and 120, and these results are in good agreement with the findings of other works [8,11–13]. Bai et al. [8] showed that the values of the interaction for the storage of a Li atom in C_{20-70} fullerenes were all negative by using DFT calculations, which was also shown by our results. In addition, our results for the distance η of Li@C_{60} were consistent with those provided by [12] with minor differences; they reported that the most energetically favorable configuration was when the displacement of the Li atom was 1.54 Å from the fullerene's center by using DFT calculations. The method and results presented in this study may offer an engineering estimation procedure for the design of batteries using fullerenes; the merit of the continuum approximation is that the Li storage capacity of fullerenes of any size can be predicted, which may be computationally challenging when applying DFT or molecular calculations. We comment that the method and results provided only the theoretical design of the interaction energies of a lithium atom stored in a C_N fullerene; further research should investigate the adsorption energies and the changes in the electronic structures of the adsorption configurations for the interactions of lithium atoms with carbon nanomaterials, including fullerenes.

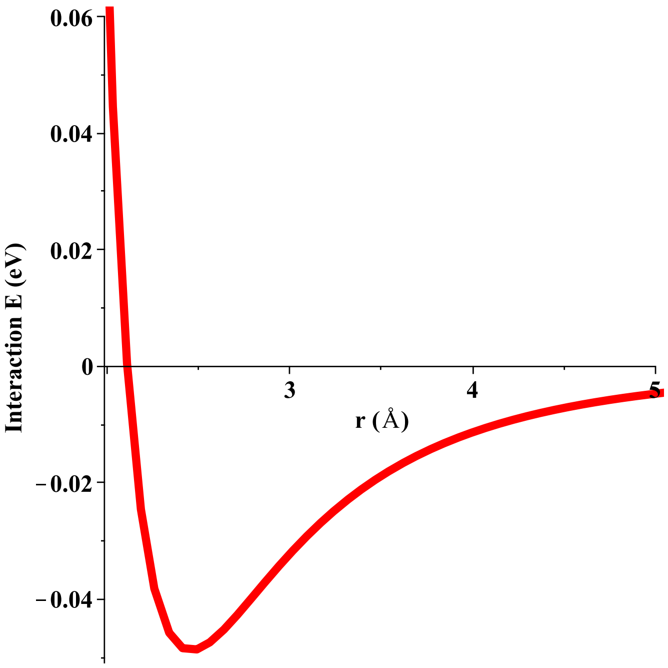

Figure 5. Total interaction between a Li atom and a fullerene as a function of the fullerene's radius r.

4. Summary

In this study, classical applied mathematics and mechanics were used to adopt the continuum approximation with the 6–12 LJ potential function in order to model the interaction energies involved in the storage of a Li atom in fullerenes of different sizes for various battery designs that use C_N fullerenes. Analytical expressions were derived to understand the process of storing lithium in fullerene molecules. With different physical parameters, our theoretical method rapidly yields numerical results for different sizes of C_N fullerenes. The results showed that Li atoms can be encapsulated in a C_N fullerene with a radius that is larger than 2 Å, and the preferred C_N for storing a Li atom is C_N with a radius of ≈2.4 Å, where the minimal interaction energy is obtained. The results presented here are shown to be in a good agreement with the results obtained by other authors in [8,11–13], who proposed that Li atoms may be encapsulated inside C_N fullerenes of different sizes, where $N \geq 20$. Overall, carbon nanomaterials—including fullerenes—can offer a well-suited playground for optimizing the nano-structure, capacity, and rated performance when using lithium storage for anode materials in Li-ion batteries. Our results can help provide a proper understanding of the encapsulation of lithium in other carbon nanomaterials, and the method adopted here can be extended in order to gain insight into this metal's storage in other molecular containers.

Funding: This project was supported by Researchers Supporting Project number (RSP2022R411), King Saud University, Riyadh, Saudi Arabia.

Data Availability Statement: Not applicable.

Conflicts of Interest: The author declares that there is no conflict of interest.

References

1. Kaskhedikar, N.A.; Maier, J. Lithium Storage in Carbon Nanostructures. *Adv. Mater.* **2009**, *21*, 2664–2680 [CrossRef]
2. Dresselhaus, M.S.; Dresselhaus, G.; Avouris, P. *Carbon Nanotubes: Synthesis, Structure, Properties and Applications*; Springer: Berlin, Germany, 2001; Volume 80.
3. Dresselhaus, M.S.; Dresselhaus, G.; Eklund, P.C. *Science of Fullerenes and Carbon Nanotubes*; Academic Press: New York, NY, USA, 1996.
4. Baowan, D.; Cox, B.J.; Hilder, T.A.; Hill, J.M.; Thamwattana, N. *Modelling and Mechanics of Carbon-Based Nanostructured Materials*, 1st ed.; William Andrew: Norwich, NY, USA, 2017.
5. Kroto, H.W.; Heath, J.R.; O'Brien, S.C.; Curl, R.F.; Smalley, R.E. C60: Buckminsterfullerene. *Nature* **1985**, *318*, 162–163. [CrossRef]
6. Harris, P.J.F. *Carbon Nanotubes and Related Structures*, 1st ed.; Cambridge University Press: Cambridge, UK, 2003.
7. Ansari, M.J.; Soltani, A.; Ramezanitaghartapeh, M.; Singla, P.; Aghaei, M.; Fadafan, H.K.; Khales, S.A.; Shariati, M.; Shirzad-Aski, H.; Balakheyli, H.; et al. Improved antibacterial activity of sulfasalazine loaded fullerene derivative: Computational and experimental studies. *J. Mol. Liq.* **2022**, *348*, 118083. [CrossRef]
8. Bai, H.; Gao, H.; Feng, W.; Zhao, Y.; Wu, Y. Interaction in Li@Fullerenes and Li+@Fullerenes: First Principle Insights to Li-Based Endohedral Fullerenes. *Nanomaterials* **2019**, *9*, 630. [CrossRef]
9. Ramezanitaghartapeh, M.; Achazi, A.J.; Soltani, A.; Miró, P.; Mahon, P.J.; Hollenkamp, A.F.; Musameh, M. Sustainable cyanide-C60 fullerene cathode to suppress the lithium polysulfides in a lithium-sulfur battery. *Sustain. Mater. Technol.* **2022**, *32*, e00403. [CrossRef]
10. Baei, M.T.; Taghartapeh, M.R.; Soltani, A.; Amirabadib, K.H.; Gholamib, N. Interaction of pure and metal atom substituted carbon nanocages with CNCl: A DFT study. *Russ. J. Phys. Chem. B* **2017**, *11*, 354–360. [CrossRef]
11. An, Y.; Yang, C.; Wang, M.; Ma, X.; Wang, D. Geometrical and Electronic Properties of the Clusters of C_{20} Cage Doped with Alkali Metal Atoms. *J. Clust. Sci.* **2011**, *22*, 31–39. [CrossRef]
12. Stefanou, M.; Chandler, H.J.; Mignolet, B.; Williams, E.; Nanoh, S.A.; Thompson, J.O.F.; Remacle, F.; Schaub, R.; Campbell, E.E.B. Angle-resolved photoelectron spectroscopy and scanning tunnelling spectroscopy studies of the endohedral fullerene Li@C60. *Nanoscale* **2019**, *11*, 2668–2678. [CrossRef] [PubMed]
13. Debnath, T.; Saha, J.K.; Banu, T.; Ash, T.; Das, A.K. Structural and thermodynamic aspects of $Li_n@C_x$ endohedral metallofullerenes: A DFT approach. *Theor. Chem. Acc.* **2016**, *135*, 167. [CrossRef]
14. Maitland, G.C.; Rigby, M.; Smith, E.B.; Wakeham, W.A. Intermolecular Forces–Their Origin and Determination; Clarendon Press: Oxford, UK, 1981.
15. Andrews, G.E.; Askey, R.; Roy, R. *Special Functions*; Cambridge University Press: Cambridge, UK, 1999.
16. Andre, P.; Aubreton, J.; Clain, S.; Dudeck, M.; Duffour, E.; Elchinger, M.F.; Izrar, B.; Rochette, D.; Touzani, R.; Vacher, D. Transport coefficients in thermal plasma. Applications to Mars and Titan atmospheres. *Eur. Phys. J. D* **2010**, *57*, 227–234. [CrossRef]
17. Bülow, M.; Shen, D.; Jale, S.R. Sorption equilibrium properties of nitrous oxide on low-silicon x-type zeolites. *Colloids Surfaces A Physicochem. Eng. Asp.* **2004**, *241*, 59–65. [CrossRef]
18. Kaur, S.; Sharma, A.; Sharma, H.; Mudahar, I. Structural and magnetic properties of small symmetrical and asymmetrical sized fullerene dimers. *Mater. Res. Express* **2018**, *5*, 016105. [CrossRef]

19. Sharma, A.; Kaur, S.; Sharma, H.; Mudahar, I. Electronic and magnetic properties of small fullerene carbon nanobuds: A DFT study. *Mater. Res. Express* **2018**, *5*, 065032. [CrossRef]
20. Wang, J.; Lu, H.; Fan, Y.; Li, S.D. I_h Symmetrical (4,6)-Fullerenes and Their Local Ring Aromaticity: A First Principle Study. *J. Nanomater.* **2015**, *15*, 867497.